Earth and Planetary Science Letters 310 (2011) 538–543

Contents lists available at SciVerse ScienceDirect

Earth and Planetary Science Letters

journal homepage: www.elsevier.com/locate/epsl

New insights into mantle convection true polar wander and rotational bulge readjustment

G. Cambiotti [a,*], Y. Ricard [b], R. Sabadini [a]

[a] Department of Earth Sciences, University of Milan, Via Cicognara 7, 20133, Milan, Italy
[b] Laboratoire de Géologie de Lyon (LGLTPE), CNRS, Université de Lyon 1, ENSL Bat Géode, 2 rue Raphæl Dubois, France

ARTICLE INFO

Article history:
Received 1 June 2011
Received in revised form 2 August 2011
Accepted 8 August 2011
Available online 5 October 2011

Editor: T. Spohn

Keywords:
rotation
inertia
mantle dynamics
geoid
true polar wander

ABSTRACT

The Earth's rotation axis is constantly tracking the main inertia axis of the planet that evolves due to internal and surface mass rearrangements. This motion called True Polar Wander (TPW) is due to mantle convection on the million years time scale. Most studies assumed that on this long time scale the planet readjusts without delay and that the Earth's rotation axis and the Maximum Inertia Direction of Mantle Convection (MID-MC) coincide. We herein overcome this approximation that leads to inaccurate TPW predictions and we provide a new treatment of Earth's rotation discussing both analytical and numerical solutions. We obtain an average TPW rate in the range $[0.5°–1.5°]\,\mathrm{Myr}^{-1}$ and a sizeable offset of several degrees between the rotation axis and the MID-MC. This is in distinct contrast with the general belief that these two axes should coincide or that the delay of the readjustment of the rotational bulge can be neglected in TPW studies. We thus clarify a fundamental issue related to mantle mass heterogeneities and to TPW dynamics.

1. Introduction

True polar wander, the slow motion of Earth's rotation axis with respect to the mantle is generally taken as evidence of mantle convection (Spada et al., 1992) and Pleistocene ice sheet melting (Cambiotti et al., 2010; Mitrovica et al., 2005; Sabadini and Peltier, 1981). Owing to the ability of the rotational bulge to relax and readjust to perturbations of the rotation axis on a time scale T that ranges from 1 to 100 kyr, depending on the internal viscoelastic stratification (Ricard et al., 1993a), Earth's rotation axis constantly tracks the Maximum Inertia Direction of Mantle Convection (MID-MC) on the million year time scale of mantle convection. On this long time scale, however, it is often assumed that the planet readjusts without delay and that the rotation axis and the MID-MC coincide (Jurdy, 1978; Rouby et al., 2010; Steinberger and O'Connell, 1997).

This coincidence, however, cannot be taken as a general rule. Using mantle density anomalies observed by seismic tomography, Ricard and Sabadini (1990) showed out that the present-day rotation axis lags behind the MID-MC by some degrees. Ricard et al. (1993a) pointed out that the planet, submitted to a change of inertia of order E attributable to mantle convection, will wander with a characteristic time of order $T(C-A)/E$, with C and A being the polar and equatorial inertia moments. In view of this, the Earth can shift its rotation pole from a starting position to a new position in a time larger than a few 100 kyr or a few million years. On the basis of similar arguments, Steinberger and O'Connell (1997) estimated that the offset between the rotation axis and the MID-MC should be less than 1°, even for an high viscous mantle with lower mantle viscosity of 10^{23} Pas. This estimate, however, was obtained assuming a MID-MC rate less than 0.2°/Myr during the past 50 Myr. Accounting for the delay of the readjustment of the rotational bulge and allowing for an offset between the geographic north pole and the present-day MID-MC, Richards et al. (1997) estimated TPW paths for different viscosity profiles of the mantle. Nevertheless, they did not quantify the offset and concluded that the influence of the delay on TPW is small.

In light of this, although Ricard et al. (1993a), Richards et al. (1997) and Steinberger and O'Connell (1997) provided some insights into the long time scale rotational behavior of the Earth, a concise and complete picture of the problem is still lacking at the moment. We herein overcome these limitations and discuss a new treatment of the non-linear Liouville equation that allows to describe the long time scale rotational behavior of the Earth via a simple linear theory. Thus, we clarify this long debated issue and its connections with seismic tomography.

2. Theory

To clarify the long time scale rotational behavior of the Earth, we must start with the basic laws governing the relative motion of the rotation axis with respect to the MID-MC. It can be appropriately dealt

* Corresponding author.
E-mail addresses: gabriele.cambiotti@unimi.it, agabrie@libero.it (G. Cambiotti), ricard@ens-lyon.fr (Y. Ricard), roberto.sabadini@unimi.it (R. Sabadini).

0012-821X/$ – see front matter © 2011 Elsevier B.V. All rights reserved.
doi:10.1016/j.epsl.2011.08.009

with in the reference frame defined by the three eigenvectors e_k of mantle convection inertia tensor $\mathcal{C}$

$$\mathcal{C} = \sum_{k=1}^{3} C_k \boldsymbol{e}_k \otimes \boldsymbol{e}_k \tag{1}$$

where $\otimes$ stands for the algebraic product and where C_k are the inertia moments. Here C_3 is the maximum inertia moment ($C_3 \geq C_2$ and $C_3 \geq C_1$) and $\boldsymbol{e}_3$ is the MID-MC. This is a time dependent reference frame and, from geometric considerations (Ben-Menahem and Singh, 1981), the time derivatives of the eigenvectors $\boldsymbol{e}_k$ yield

$$\frac{d\boldsymbol{e}_k}{dt} = \boldsymbol{\xi} \times \boldsymbol{e}_k \tag{2}$$

Here, $\boldsymbol{\xi}$ is the angular velocity of the mantle convection inertia that we write as follows

$$\boldsymbol{\xi} = -V_2 \boldsymbol{e}_1 + V_1 \boldsymbol{e}_2 + V_3 \boldsymbol{e}_3 \tag{3}$$

in such a way that V_1 and V_2 are the components of the MID-MC velocity $d\boldsymbol{e}_3/dt$ along the equatorial axes $\boldsymbol{e}_1$ and $\boldsymbol{e}_2$, respectively. V_3 describes the counterclockwise rotation rate of the equatorial axes around the MID-MC.

We write Earth's angular velocity $\boldsymbol{\omega}$ as $\boldsymbol{\omega} = \omega \boldsymbol{n}$, where ω and $\boldsymbol{n}$ are the rotation rate and axis. Within the reasonable assumption that the angle between rotation axis and MID-MC is small, the rotation axis $\boldsymbol{n}$ can be expressed in terms of direction cosines m_1 and m_2 along the equatorial axes $\boldsymbol{e}_1$ and $\boldsymbol{e}_2$,

$$\boldsymbol{n} = m_1 \boldsymbol{e}_1 + m_2 \boldsymbol{e}_2 + \boldsymbol{e}_3. \tag{4}$$

The time variation of Earth's angular velocity $\boldsymbol{\omega}$ is therefore

$$\frac{d\boldsymbol{\omega}}{dt} = \boldsymbol{n}\frac{d\omega}{dt} + \omega \frac{d\boldsymbol{n}}{dt} \tag{5}$$

where the first term on the right is related to the change of the length of the day and the second term to the TPW velocity $\boldsymbol{v} = d\boldsymbol{n}/dt$, which, assuming that the time evolution of mantle convection is slow, becomes

$$\boldsymbol{v} = \left(\frac{dm_1}{dt} + V_1\right)\boldsymbol{e}_1 + \left(\frac{dm_2}{dt} + V_2\right)\boldsymbol{e}_2. \tag{6}$$

The expressions (4) and (6) are correct to first order, for small m_1, m_2 and $\boldsymbol{\xi}$ (i.e., neglecting terms of order $m_i m_j$ or $m_i V_j$).

The rotation axis, averaged over a few Chandler periods, is aligned with the direction of maximum total inertia (Munk and MacDonald, 1960), i.e., is the eigenvector of the sum of the inertia tensors due to the rotational bulge, $\mathcal{B}$, and the mantle convection, $\mathcal{C}$,

$$\boldsymbol{n} \times (\mathcal{B} + \mathcal{C}) \cdot \boldsymbol{n} = \boldsymbol{0}. \tag{7}$$

We take into account the relaxation of rotational bulge by means of the long-term approximation (Ricard et al., 1993a; Spada et al., 1992) of MacCullagh's formula for centrifugal deformation (Munk and MacDonald, 1960). As shown in Appendix A, it can be cast as follows

$$\mathcal{B} = \beta \omega^2 \left[\left(1 - \frac{2T}{\omega}\frac{d\omega}{dt}\right)\left(\boldsymbol{n}\otimes\boldsymbol{n} - \frac{1}{3}\boldsymbol{1}\right) - T(\boldsymbol{n}\otimes\boldsymbol{v} + \boldsymbol{v}\otimes\boldsymbol{n})\right] \tag{8}$$

where $\boldsymbol{1}$ is the identity matrix, T the time scale of readjustment of rotational bulge and $\beta\omega^2$ the difference between polar and equatorial inertia moments of the hydrostatic rotational bulge. The time scale T can easily be computed for any spherically symmetric viscoelastic Earth's model and should be of the order of 30 kyr (Ricard et al., 1993a).

Eq. (6) accounts for the readjustment of the rotational bulge due to variations of the length of day via the term proportional to $d\omega/dt$. However, as we have neglected the time derivative of the angular momentum in the Liouville equation averaged over a few Chandler periods (see Eq. (7)), the length of day remains constant and the minute term $(2T/\omega)(d\omega/dt)$ can also be neglected.

Thus, by solving Eq. (7) using Eqs. (1), (4), (6) and (8), we obtain a first order differential equation for each direction cosine m_i

$$\frac{dm_i}{dt} + \frac{m_i}{T_i} = -V_i \qquad (i = 1,2) \tag{9}$$

where T_i are time scales defined by

$$T_i = \frac{\beta\omega^2}{C_3 - C_i} T \qquad (i = 1,2) \tag{10}$$

Eqs. (9) and (10) show that V_i are the forcings of the relative motion of rotation axis and that the actual time scales T_i controlling this relative motion are not simply the time scale T of the rotational bulge readjustment, but are increased by the factor $\beta\omega^2/(C_3 - C_i)$.

The difference between polar and equatorial inertia moments of the hydrostatic rotational bulge $\beta\omega^2$ has been recently estimated (Chambat et al., 2010)

$$\beta\omega^2 \approx 1.0712 \times 10^{-3} Ma^2 \tag{11}$$

with M and a being the Earth's mass and mean radius. The differences between the inertia moments of mantle convection, $C_3 - C_i$, is typically of order of the differences between the observed total inertia moments of the Earth (usually defined as A, B and C), minus the hydrostatic contribution $\beta\omega^2$ (Chambat & Valette, 2001)

$$\begin{aligned} C_3 - C_1 &\approx (C-A) - \beta\omega^2 = 1.48 \times 10^{-5} Ma^2 \\ C_3 - C_2 &\approx (C-B) - \beta\omega^2 = 0.78 \times 10^{-5} Ma^2. \end{aligned} \tag{12}$$

Thus, as already argued in Ricard et al. (1993a), the time scales T_i are greater than T by a factor of about 100. Assuming $T = 30$ kyr, the relative motion of rotation axis is controlled by time scales $T_i \approx 3$ Myr, that are comparable with those of mantle convection, say greater than 1 Myr. These findings show that the previous approximation based on the assumption that the rotational bulge readjusts instantaneously to perturbations of the rotation axis is not accurate. Particularly, it missed a fundamental aspect of TPW dynamics: the inertia perturbations due to mantle convection are two orders of magnitude smaller than those of the rotational bulge. Such a smallness increases the time scales for viscoelastic readjustment of the rotational bulge during the TPW to values comparable to those of mantle convection. Notice also that the two direction cosines m_1 and m_2 behave differently as T_1 and T_2 are likely to differ due to dependence in Eq. (10) on the differences $C_3 - C_1$ and $C_3 - C_2$ (they differ by a factor of 2 at the present-day). Furthermore, since the time scales T_i are evolving with time, they could potentially become infinite during inertial interchanges (Richards et al., 1999), a case that would invalidate our linearized approach.

The role of the time scales T_i becomes clear by assuming them constant. In this case, the solution of the linearized Earth's rotation differential equations, Eq. (9), yields

$$m_i(t) = -e^{-t/T_i} \bigstar V_i \qquad (i = 1,2) \tag{13}$$

with $\bigstar$ standing for time convolution. This means that the time scales T_i are the relaxation times for the relative motion of the rotation pole forced by the MID-MC velocity components V_i. In this respect, Eq. (9) and its particular solution, Eq. (13), allow us to discern the effects on TPW dynamics due to the delay of the readjustment of the rotational

bulge and to the time evolution of mantle convection. A MID-MC velocity, constant for a time greater than T_i, drives the pole at the same velocity, $dm_i/dt = 0$, but with the pole lagging behind the MID-MC by the angle

$$m_i = -T_i V_i \qquad (i = 1,2). \tag{14}$$

This result has the same physical meaning as Eq. (1) of Steinberger and O'Connell (1997). Furthermore, from Eq. (13), it is also clear that variations of the MID-MC velocity, occurring on times comparable or smaller than T_i, break the equilibrium of the relative position of the rotation axis with respect to the MID-MC given by Eq. (14). Particularly, they yield different TPW and MID-MC velocity amplitudes and directions. Such a result cannot be inferred within the previous framework (Ricard et al., 1993a; Richards et al., 1997; Steinberger and O'Connell, 1997) and shows that estimates of TPW rates must account both for fluctuations of Earth's inertia tensor and the delay of readjustment of rotational bulge.

3. Time-dependent inertia due to mantle convection

Let us consider the components $\mathcal{C}_{ij} = \boldsymbol{x}_i \cdot \boldsymbol{\mathcal{C}} \cdot \boldsymbol{x}_j$ and $\mathcal{B}_{ij} = \boldsymbol{x}_i \cdot \boldsymbol{\mathcal{B}} \cdot \boldsymbol{x}_j$ of the mantle convection and rotational bulge inertia tensors in the geographical reference frame with unit vectors $\boldsymbol{x}_1, \boldsymbol{x}_2$ and $\boldsymbol{x}_3$ ($\boldsymbol{x}_1$ points to the equator and the Greenwich meridian, while $\boldsymbol{x}_3$ points to the north pole, i.e., coincides with the present-day rotation axis). In view of Eq. (7), at present time $t = 0$, the total inertia tensor (mantle convection plus rotational bulge) has zero off-diagonal components along $\boldsymbol{x}_3$

$$\mathcal{C}_{i3}(0) + \mathcal{B}_{i3}(0) = 0 \qquad (i = 1,2) \tag{15}$$

and, by making use of Eq. (8), we obtain

$$\mathcal{C}_{i3}(0) = \beta\, \omega^2 T\, \boldsymbol{x}_i \cdot \boldsymbol{v}(0) \qquad (i = 1,2) \tag{16}$$

which corresponds to Eqs. (8)–(9) of Ricard et al. (1993b) or Eq. (3) of Steinberger and O'Connell (1997). Thus, the off-diagonal components $\mathcal{C}_{13}(0)$ and $\mathcal{C}_{23}(0)$ of the mantle convection inertia tensor are non-zero in a wandering planet (i.e., when $\boldsymbol{v}(0) \neq \boldsymbol{0}$) and cannot be estimated from observations of the total inertia of the Earth as they are compensated by the rotational bulge not yet readjusted to the north pole. They must be estimated from 3-D models of Earth's density anomalies, accounting for the effect of dynamic topography (Ricard et al., 1993b), or by solving the rotational problem as we are going to show.

We compute the mantle convection inertia tensor by means of our previously developed modeling strategy (Ricard et al., 1993b; Richards et al., 1997), assuming that largest changes in mantle density heterogeneities are likely caused by subduction. We use reconstructions of global plate motions for Cenozoic and late Mesozoic (Lithgow-Bertelloni et al., 1993), to inject cold slabs into the mantle where plates converge. In order to account for present-day geoid, for much of the observed seismic heterogeneities of the mantle and for the long term rotational stability of the Earth indicated by paleomagnetic data (Richards et al., 1997), we consider lower/upper mantle and lithosphere/upper mantle viscosity ratios of $\eta_1 = 30$ and $\eta_2 = 10$, respectively. The sinking velocity of slabs when they enter the lower mantle is reduced by a factor of 4.4 (the velocity decrease is expected to scale roughly with the logarithm of the viscosity increase). This relation between viscosity increase and velocity reduction is a crude estimate that neglects the complexity of thermal exchanges between the slabs and the transition zone (Otha, 2010), but it is validated by the good fit to the geoid and to the lower mantle tomography provided by the sinking slab model (Ricard et al., 1993b). Our kinematic approach is independent of any assumed absolute mantle viscosity and yields an average sinking velocity of slabs in the lower mantle of order 1.6 cm yr^{-1}. This typical sinking velocity has been confirmed by other studies (e.g., van der Meer et al., 2010).

This kinematic model of the mantle time-dependent density anomalies is certainly simple but it provides a robust estimate of the inertia tensor which is related to a radial integral of the longest wavelengths of the density anomalies (degree 2). Therefore, the details of paleo-reconstructions do not impact this model. This model should provide a better estimate of the time dependent evolution of Earth's inertia than complex dynamic models (e.g., Steinberger, 2000) that require many questionable assumptions (a backward in time advection of the present density anomalies that requires the choice of an absolute viscosity and assumes a depth dependent rheology in contradiction with the very existence of plates).

The kinematic slab model provides a time-dependent inertia tensor $\boldsymbol{\mathcal{C}}^{slab}(t)$. At present time, this model, $\boldsymbol{\mathcal{C}}^{slab}(0)$, maximizes the correlation with the observed inertia deduced from the geoid, $\boldsymbol{\mathcal{C}}^{obs}$, and is in good agreement with tomography. As discussed previously, the mantle inertia tensor $\boldsymbol{\mathcal{C}}^{obs}$ observed from geoid does not account for the two off-diagonal components along $\boldsymbol{x}_3$ that, according to Eq. (16), are related to the history of TPW. As a consequence we consider that Earth's rotation is forced by

$$\boldsymbol{\mathcal{C}}(t) = \boldsymbol{\mathcal{C}}^{slab}(t) + \boldsymbol{\mathcal{C}}^{obs} - \boldsymbol{\mathcal{C}}^{slab}(0) + \delta\boldsymbol{\mathcal{C}} \tag{17}$$

where $\delta\boldsymbol{\mathcal{C}}$ stands for the two present-day off-diagonal terms $\mathcal{C}_{13}(0)$ and $\mathcal{C}_{23}(0)$.

This inertia tensor $\boldsymbol{\mathcal{C}}(t)$ is in agreement with that observed and has a time dependence estimated from slab paleo-positions. We then constrain the two unknown terms $\mathcal{C}_{13}(0)$ and $\mathcal{C}_{23}(0)$ by solving the non-linear Liouville Eq. (7) for a given time scale T and by requiring that the present-day rotation axis $\boldsymbol{n}(0)$ coincides with the geographical north pole. In this way, the present-day total inertia $\boldsymbol{\mathcal{C}}(0) + \boldsymbol{\mathcal{B}}(0)$ has zero off-diagonal components along $\boldsymbol{x}_3$, as required by Eq. (15). Note also that the term $\boldsymbol{\mathcal{C}}^{obs} - \boldsymbol{\mathcal{C}}^{slab}(0)$ entering Eq. (17) accounts for any contribution other than slab subduction that can be assumed to remain constant with time, as large-scale upwellings (Rouby et al., 2010) and the two large low shear velocity provinces (LLSVPs) in Earth's lowermost mantle (Steinberger and Torsvik, 2010; Torsvik et al., 2006). This term is small as the slabs by themselves explain most of the geoid, which suggests that the LLSVPs should not affect significantly the inertia tensor.

This approach is somewhat similar to the method used in Richards et al. (1997) (see their note 26). However, it does not arbitrarily assume that the present-day mantle inertia terms $\mathcal{C}_{13}(0)$ and $\mathcal{C}_{23}(0)$ are zero. The latter assumption has been made in Steinberger and O'Connell (1997) or Schaber et al. (2010). It implies the coincidence between the present-day rotation axis and the MID-MC which is in contradiction with the observation of ongoing TPW as shown in Eq. (16). Instead, by solving for the two unknown terms, $\mathcal{C}_{13}$ and $\mathcal{C}_{23}$, we respect the correct physics of the problem. Notice also that we solve the Liouville equations from past (starting ~100 Myr ago) to present. It is incorrect to try to solve the Liouville equation backward in time as was done in Schaber et al. (2010) which results in rotation axis apparently preceding the MID-MC rather than lagging behind the MID-MC as it should (see their Fig. 5).

In the following, we will express the off-diagonal terms $\mathcal{C}_{13}$ and $\mathcal{C}_{23}$ of the mantle convection inertia tensor in terms of the C_{21} and S_{21} geoid coefficients in meters, that are due to mantle convection alone and would be observed in the absence rotation. They are related to each other as follows

$$\begin{aligned} \mathcal{C}_{13} &= -Ma^2 \sqrt{\frac{5}{3}} \frac{C_{21}}{a} \\ \mathcal{C}_{23} &= -Ma^2 \sqrt{\frac{5}{3}} \frac{S_{21}}{a}. \end{aligned} \tag{18}$$

4. TPW simulations

Fig. 1 compares TPW paths obtained for three time scales $T=0$, 30 and 100 kyr. The case of $T=0$ corresponds to the readjustment of the rotational bulge without delay. For viscosity ratios of $\eta_1=30$ (lower to upper mantle) and $\eta_2=10$ (lithosphere to upper mantle), the time scales $T=30$ and 100 kyr correspond to upper mantle viscosities of about 10^{21} and 3.3×10^{21} Pas, respectively (the time scale T is proportional to the upper mantle viscosity ν_M, as discussed in Ricard et al., 1993a, 1993b). As initial condition for the Liouville equation, we assume that the rotation axis coincides with the MID-MC at 100 Myr before present. However, in view of Eq. (13), it should be noticed that the TPW path is affected by the initial condition only for a time of order T_i (Fig. 2), about 3 and 9 Myr for $T=30$ and 100 Kyr.

Due to the differences in the relaxation of the rotational bulge, TPW paths differ from each other. Particularly, the polar excursion in the past 10 Myr reduces from 6.9° for $T=0$ to 5.3° and 3.6° for $T=30$ and 100 kyr, respectively. Furthermore, the present-day MID-MC occupies different positions, reflecting the estimated C_{21} and S_{21} geoid coefficients due to mantle convection driven by slab subduction (Table 1). Particularly, for $T=0$, the present-day MID-MC is at the north pole since the rotational bulge readjusts instantaneously. On the contrary, for $T=30$ and 100 kyr, the present-day MID-MC are displaced by 3.4° and 7.1° towards 68.9°E and 64.6°E, respectively.

A reduction of the polar excursion by increasing the time scale T is expected on physical grounds, once the herein developed linearized differential equations, Eqs. (9) and (13), are considered to reinterpret the non-linear calculations. For the three time scales $T=0,30$ and 100 kyr, Fig. 3 compares the MID-MC and TPW rates. For $T=0$, the rotational bulge readjusts instantaneously and, thus, the MID-MC and TPW rates and paths coincide. Particularly, the TPW rate is affected by every short-term fluctuation of Earth's inertia tensor. Instead, for $T=30$ and 100 kyr, the inhibition of the bulge relaxation filters out in time the short-term fluctuations of Earth's inertia, thus smoothing TPW rates. Furthermore, accordingly to Eq. (13), variations of TPW rates are delayed with respect to those of MID-MC by a time comparable to the time scales T_i (Fig. 2). Particularly, this yields a reduction of the present-day TPW rate since the MID-MC rate increases by about 1 Myr^{-1} in the past 10 Myr. Compared to the present-day TPW rate of 1.24 Myr^{-1} for $T=0$, the present-day TPW rates of 0.85 and 0.55 Myr^{-1} for $T=30$ and 100 kyr, respectively, are reduced by 32 and 56%.

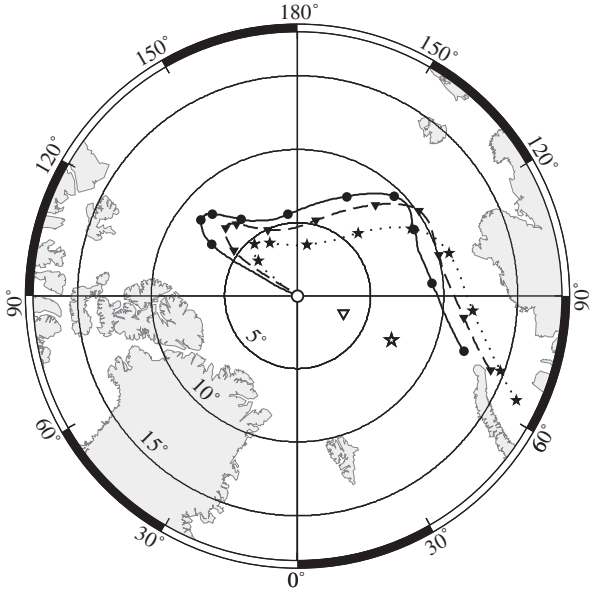

Fig. 1. TPW paths for three time scales $T=0$, 30 and 100 kyr (solid, dashed and dot lines with circles, triangles and stars, respectively). The symbols are given at intervals of 10 Myr. The present-day MID-MC positions for three time scales $T=0,30$ and 100 kyr are also shown (open circles, triangles and stars, respectively). Only when the rotational bulge readjusts instantaneously ($T=0$), the MID-MC coincides with the north pole.

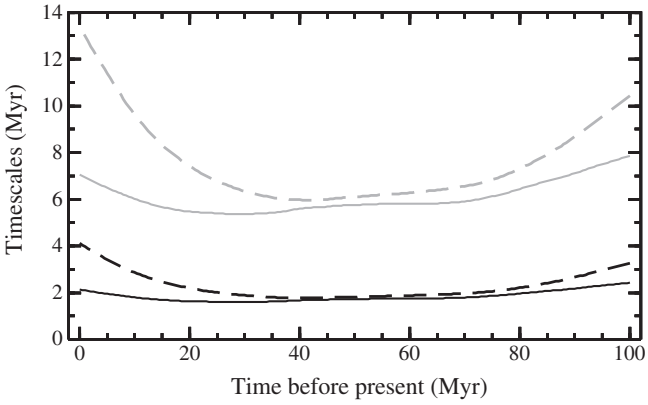

Fig. 2. Time scales T_1 and T_2 (solid and dashed lines, respectively) controlling the relative motion of the rotation axis with respect to the MID-MC, Eq. (10), for the time scale $T=30$ and 100 kyr (black and gray lines, respectively).

Together with the TPW rate decrease, the offset angle between the rotation axis and the MID-MC increases, see Fig. 4. For $T=30$ and 100 kyr, they are about 0.8 and 2.2 in the past 100 Myr and they increase to 3.4 and 7.1 at the present-day due to the acceleration of the MID-MC in the past 10 Myr. Differently, the present-day TPW directions are only slightly affected by the readjustment of rotational bulge (Fig. 1) and they point towards 66.7°E, 61.5°E and 55.7°E for $T=0,30$ and 100 kyr, respectively. Even though the estimated TPW rates are in rough agreement with the observation of 0.925 ± 0.022°Myr^{-1} (McCarthy and Luzum, 1996), these results are in contrast with the observed direction towards Newfoundland (75.0 ± 1.1°W). The general motion since the early Tertiary (50 to 60 Myr) of about 4° − 9° toward Greenland is however in agreement with paleomagnetic data (Besse and Courtillot, 2002), although we do not obtain the period of (quasi) standstill at 10 − 50 Myr.

5. Conclusion

We have reinterpreted TPW simulations on the basis of the linearization of the Liouville equation provided in Eq. (9). Discerning between the effects of the delay of the readjustment of the rotational bulge from those of the specific mantle convection models used in TPW simulations, we have pointed out when the former can affect significantly both TPW path and rates. By implementing a previously developed mantle circulation model (Ricard et al., 1993b; Richards et al., 1997), we have shown that the delay of the readjustment of the rotational bulge can shift the TPW and MID-MC paths by several degrees and affects present-day TPW rates by about 50%.

Table 1
Present-day C_{21} and S_{21} geoid coefficients due to mantle convection estimated from seismic tomography (top line, coefficients obtained using the tomographic model Smean of Becker & Boschi (2002) as described in Ricard et al., 1993b) or self-consistently estimated from TPW dynamics driven by the model of subduction, for the three time scales $T=0,30$ and 100 kyr (bottom lines).

Geoid coefficients (m)	C_{21}	S_{21}
Seismic tomography	−1.00	0.53
TPW dynamics ($T=0$ kyr)	0	0
TPW dynamics ($T=30$ kyr)	1.05	−2.07
TPW dynamics ($T=100$ kyr)	−2.87	−4.19

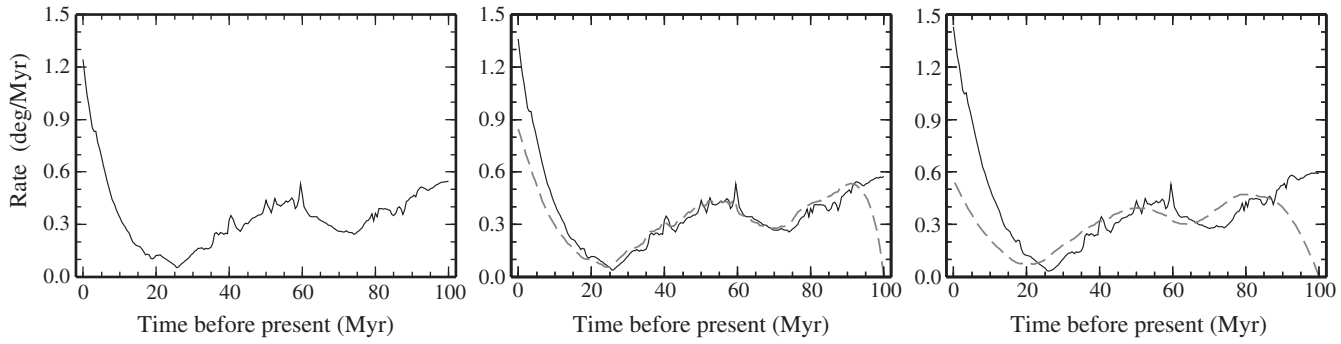

Fig. 3. MID-MC, $|d\boldsymbol{e}_3/dt|$, and TPW, $|\boldsymbol{v}|$, rates (solid and dashed lines, respectively) for the three time scales $T=0$, 30 and 100 kyr (left, middle and right panels, respectively). The MID-MC and TPW rates coincide for $T=0$. The TPW rates for $T=30$ and 100 kyr are zero at 100 Myr before present since we have imposed as initial condition that the rotation axis andthe MID-MC coincide at that time. The TPW simulations do no longer depend on the initial condition after a time comparable with the time scales T_i (Fig. 2).

The slow change of the mantle convection inertia tensor remains the main factor explaining the long-term rotational stability of the Earth (Richards et al., 1997). However, as clearly indicated by Eqs. (9) and (13), the relaxation of the rotational bulge introduces a further stabilizing effect. Indeed, it filters out every short-term fluctuations of the Earth's inertia tensor and delays variations of TPW rates by the time scales T_i, Eq. (10), with respect to those of the MID-MC. This yields significant differences between TPW and MID-MC rates, particularly during the past 10 Myr for our mantle convection model.

In addition to slab subduction, we have accounted also for any other contributions to mantle density anomalies that can be assumed to remain constant with time. Furthermore, the present-day C_{21} and S_{21} geoid coefficients due to mantle density anomalies alone, which cannot be observed since they are compensated by the rotational bulge not yet readjusted to the north pole, have been estimated self-consistently with TPW dynamics. Within our framework, it is possible to check if TPW simulations are in agreement with seismic tomography. By using in Eqs (16) and (18) the C_{21} and S_{21} geoid coefficients obtained from the tomographic model Smean of Becker & Boschi (2002) (see Table 1) which is an average of various recent models, we obtain a present-day TPW direction of 28°W, in rough agreement with the observed direction towards Newfoundland, and a present-day TPW rate of $0.0123°/T$, inversely proportional to the time scale T (the observed TPW rate of $0.925\pm0.22°\text{Myr}^{-1}$ is explained when $T=13$ kyr). Nevertheless, these estimates concern only the present-day and are not consistent with TPW simulations obtained using the time evolution of mantle convection inferred from global plate motions (Ricard et al., 1993b; Lithgow-Bertelloni et al., 1993).

The combined use of seismic tomography and reconstructions of global plate motions could greatly improve our understanding of both past and present-day TPW driven by mantle convection. However, these two data sets cannot be used contemporarily to simulate TPW if the delay of the rotational bulge is accounted for. Furthermore, in order to fulfill observations, the contribution to TPW from Pleistocene ice sheet melting must be also considered, being comparable in magnitude with that from mantle convection and pointing towards Newfoundland (Cambiotti et al., 2010; Mitrovica et al., 2005). Because it occurs on a much shorter period than mantle convection, the deglaciation affects the TPW, but its contribution to Earth's inertia tensor remains negligible compared to that of the mantle 3-D structure.

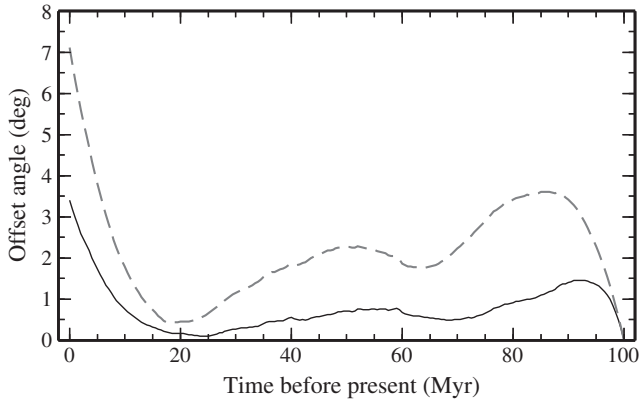

Fig. 4. Offset angle, $\arccos(\boldsymbol{n}\cdot\boldsymbol{e}_3)$, between the rotation axis and the MID-MC for the time scales $T=30$ and 100 kyr (solid and dashed lines, respectively). For $T=0$ the offset angle is zero at any time since the rotational bulge readjusts instantaneously.

Acknowledgments

We thank David Yuen for important discussions. This work is supported by GOCE-Italy project by ASI (Italian Space Agency).

Appendix A. Proof of Eq. (7) for the rotational bulge

The long-term approximation of the MacCullagh's formula given in Eq. (10) of Ricard et al. (1993a) can be written in the dyadic formulation (Ben-Menahem and Singh, 1981) as follows

$$\mathcal{B}=\beta\left[\left(\omega_j\omega_k-\frac{1}{3}\omega^2\delta_{jk}\right)-T\left(\dot{\omega}_j\omega_k+\omega_j\dot{\omega}_k-\frac{2}{3}\omega_p\dot{\omega}_p\delta_{jk}\right)\right]\boldsymbol{x}_j\otimes\boldsymbol{x}_k \tag{A.1}$$

where $\boldsymbol{x}_j$ and ω_j are the unit vectors of the geographical reference frame and the respective components of Earth's angular velocity $\boldsymbol{\omega}$

$$\boldsymbol{\omega}=\omega\,\boldsymbol{n}=\omega_i\boldsymbol{x}_i \tag{A.2}$$

and

$$\beta=k_F^T\,a^5/(3\,G) \tag{A.3}$$

with k_F^T being the degree-2 tidal gravitational fluid limit (Cambiotti et al., 2010; Chambat et al., 2010). The time derivative of Eq. (A.2) yields

$$\dot{\boldsymbol{\omega}}=\dot{\omega}\boldsymbol{n}+\omega\boldsymbol{v}=\dot{\omega}_i\boldsymbol{x}_i \tag{A.4}$$

By making use of the algebra of the dyadics (Ben-Menahem and Singh, 1981), we note that

$$\omega_j\omega_k\boldsymbol{x}_j\otimes\boldsymbol{x}_k=\boldsymbol{\omega}\otimes\boldsymbol{\omega}=\omega^2\boldsymbol{n}\otimes\boldsymbol{n} \tag{A.5}$$

$$\omega^2\delta_{jk}\boldsymbol{x}_j\otimes\boldsymbol{x}_k=\omega^2\mathbf{1} \tag{A.6}$$

$$\dot{\omega}_j\omega_k\boldsymbol{x}_j\otimes\boldsymbol{x}_k=\dot{\boldsymbol{\omega}}\otimes\boldsymbol{\omega}=\omega\dot{\omega}\boldsymbol{n}\otimes\boldsymbol{n}+\omega^2\boldsymbol{v}\otimes\boldsymbol{n} \tag{A.7}$$

$$\dot{\omega}_k\omega_j\boldsymbol{x}_j\otimes\boldsymbol{x}_k=\boldsymbol{\omega}\otimes\dot{\boldsymbol{\omega}}=\omega\dot{\omega}\boldsymbol{n}\otimes\boldsymbol{n}+\omega^2\boldsymbol{n}\otimes\boldsymbol{v} \tag{A.8}$$

$$\omega_p \dot{\omega}_p \delta_{jk} \boldsymbol{x}_j \otimes \boldsymbol{x}_k = \omega \dot{\omega} \mathbf{1} \tag{A.9}$$

Thus, the two quantities within the round brackets of Eq. (A.1) can be cast as follows

$$\left(\omega_j \omega_k - \frac{1}{3}\omega^2 \delta_{jk}\right) \boldsymbol{x}_j \otimes \boldsymbol{x}_k = \omega^2 \left(\boldsymbol{n} \otimes \boldsymbol{n} - \frac{1}{3}\mathbf{1}\right) \tag{A.10}$$

$$\begin{aligned} &\left(\dot{\omega}_j \omega_k + \omega_j \dot{\omega}_k - \frac{2}{3}\omega_p \dot{\omega}_p \delta_{jk}\right) \boldsymbol{x}_j \otimes \boldsymbol{x}_k \\ &= 2\omega\dot{\omega}\left(\boldsymbol{n} \otimes \boldsymbol{n} - \frac{1}{3}\mathbf{1}\right) + \omega^2 (\boldsymbol{v} \otimes \boldsymbol{n} + \boldsymbol{n} \otimes \boldsymbol{v}) \end{aligned} \tag{A.11}$$

and, by using these results in Eq. (A.1), we obtain Eq. (8).

References

Becker, T.W., Boschi, L., 2002. A comparison of tomographic and geodynamic mantle models. Geochem. Geophys. Geosyst. 3, 2001GC000168.

Ben-Menahem, A., Singh, S.J., 1981. Seismic Waves and Sources. Springer-Verlag, New York, Heidelberg, Berlin, pp. 946–950.

Besse, J., Courtillot, V., 2002. Apparent and true polar wander and the geometry of the geomagnetic field over the last 200 Myr. J. Geophys. Res. 107, 2300.

Cambiotti, G., Ricard, Y., Sabadini, R., 2010. Ice age true polar wander in a compressible and non-hydrostatic Earth. Geophys. J. Int. 183, 1248–1264.

Chambat, F., Valette, B., 2001. Mean radius, mass, and inertia for reference Earth models. Phys. Earth Planet. Inter. 124, 237–253.

Chambat, F., Ricard, Y., Valette, B., 2010. Flattening of the Earth: further from hydrostaticity than previously estimated. Geophys. J. Int. 183, 727–732.

Jurdy, D.M., 1978. An alternative model for early Tertiary absolute plate motions. Geology 6, 469–472.

Lithgow-Bertelloni, C., Richards, M.A., Ricard, Y., O'Connell, R., Engebreston, D.C., 1993. Torodial-Poloidal partitioning of plate motions since 120 MA. Geophys. Res. Lett. 20, 375–378.

McCarthy, D.D., Luzum, J.B., 1996. Path of the mean rotational pole from 1899 to 1994. Geophys. J. Int. 125, 623–629.

Mitrovica, J.X., Wahr, J., Matsuyama, I., Paulson, A., 2005. The rotational stability of an ice-age earth. Geophys. J. Int. 161, 491–506.

Munk, W.H., MacDonald, G.J.F., 1960. The Rotation of the Earth: A Geophysical Discussion. Cambridge University Press, London, New York, Melbourne, pp. 24–26.

Otha, K., 2010. Electrical and Thermal Conductivity of the Earth's Lower Mantle, PhD. Thesis, Tokyo Institute of Technology.

Ricard, Y., Sabadini, R., 1990. Rotational instabilities of the Earth induced by mantle density anomalies. Geophys. Res. Lett. 17, 627–630.

Ricard, Y., Spada, G., Sabadini, R., 1993a. Polar wandering of a dynamic Earth. Geophys. J. Int. 113, 284–298.

Ricard, Y., Richards, M.A., Lithgow-Berteloni, C., Le Stunff, Y., 1993b. A geodynamic model of mantle mass heterogeneities. J. Geophys. Res. 98, 21.895–21.909.

Richards, M.A., Ricard, Y., Lithgow-Bertelloni, C., Spada, G., Sabadini, R., 1997. An explanation for Earth's long-term rotational stability. Science 275, 372–375.

Richards, M.A., Bunge, H.-P., Ricard, Y., Baumgardner, J.R., 1999. Polar wandering in mantle convection models. Geophys. Res. Lett. 26, 1777–1780.

Rouby, H., Greff-Lefftz, M., Besse, J., 2010. Mantle dynamics, geoid, inertia and TPW since 120 Myr. Earth Planet. Sci. Lett. 292, 301–311.

Sabadini, R., Peltier, W.R., 1981. Pleistocene deglaciation and the Earth's rotation: implication for mantle viscosity. Geophys. J. R. Astron. Soc. 66, 553–578.

Schaber, K., Bunge, H.-P., Schubert, B.S.A., Malservisi, R., Horbach, A., 2010. Stability of the rotation axis in high-resolution mantle circulation models: weak polar wander despite strong core heating. Geochem. Geophys. Geosyst. 10, Q11W04.

Spada, G., Ricard, Y., Sabadini, R., 1992. Excitation of true polar wander by subduction. Nature 360, 452–454.

Steinberger, B., O'Connell, J., 1997. Changes of the Earth's rotation axis owing to advection of mantle density heterogeneities. Nature 387, 169–173.

Steinberger, B., 2000. Slabs in the lower mantle - results of dynamic modelling compared with tomographic images and the geoid. Phys. Earth Planet. Inter. 118, 241–257.

Steinberger, B., Torsvik, T.H., 2010. Toward an explanation for the present and past locations of the poles. Geochem. Geophys. Geosyst. 11, Q06W06.

Torsvik, T.H., Smethurst, M.A., Borke, K., Steinberger, B., 2006. Large igneous provinces generated from the margins of the large low-velocity provinces in the deep mantle. Geophys. J. Int. 167, 1447–1460.

van der Meer, D.G., Spakman, W., van Hinsbergen, D.J.J., Amaru, M.L., Torsvik, T.H., 2010. Towards absolute plate motions constrained by lower-mantle slab remnants. Nat. Geosci. 3, 36–40.